



A MPPT strategy with variable weather parameters through analyzing the effect of the DC/DC converter to the MPP of PV system



Shaowu Li^{a,b,*}, Honghua Liao^a, Hailing Yuan^a, Qing Ai^a, Kunyi Chen^a

^a School of Information Engineering, Hubei University for Nationalities, Enshi, China

^b Science and Technology College of Hubei University for Nationalities, Enshi, China

ARTICLE INFO

Article history:

Received 5 July 2016

Received in revised form 12 December 2016

Accepted 3 January 2017

Keywords:

PV system

MPPT

VWP

MPP

DC/DC converter

ABSTRACT

In order to achieve the maximum power point (MPP) of photovoltaic (PV) system as quickly as possible and improve the MPPT adaptability to the varying weather conditions, in this paper, a maximum power point tracking (MPPT) control strategy with variable weather parameters (VWP) is proposed. In this strategy, the MPP difference between PV system with and without DC/DC converter is analyzed and used as the theoretical basis of acquiring the MPP control signal. Meanwhile, the direct relationship between control signal and VWP is found out by the curve-fitting technique, which is the key work to implement this proposed strategy. Finally, some simulation experiments show that the proposed control strategy is feasible and available to track the MPP successfully, and has better MPPT performance than conventional perturbation and observation (P&O) method under different weather conditions and than fuzzy control method under fast changing weather conditions.

© 2017 Elsevier Ltd. All rights reserved.

1. Introduction

Now almost all PV systems use the MPPT technique to avoid the produced power losses. These methods or strategies for MPPT control are mainly include the constant voltage tracking (Mohanty et al., 2014), the P&O method (Liu et al., 2014; Ahmed and Salam, 2015; Jiang et al., 2014; Ishaque et al., 2014), the incremental conductance (IncCond) method (Ishaque et al., 2014; Sivakumar et al., 2015; Elgendy et al., 2013), the genetic algorithm (Shaiek et al., 2013; Deshkar et al., 2015), the fuzzy logic control method (Mellit and Kalogirou, 2014; Guenounou et al., 2014), the neural network method (Salam et al., 2013), the sliding mode control method (Zhang et al., 2015; Hong and Chen, 2014), the predictive control technique (Tsang and Chan, 2013), and so on. In them, the P&O method, which is regarded as the representation of classical MPPT methods, and the fuzzy control method, which is regarded as the representation of intelligent MPPT methods, have been widely used in practical application. The advantages of P&O method mainly include its low-cost hardware, easy implementa-

tion and good performance without solar irradiance and temperature varying quickly with time. However, there are also some shortcomings including its slow tracking speed and oscillation around MPP. The fuzzy control method mainly has the good performance under fast changing weather conditions while carrying its high-cost processor and its difficult acquisition of empirical data. In this paper, the P&O method and the fuzzy control technique are all selected as the compared object in order to study the output performance of proposed MPPT strategy.

With respect to the issue how the MPP of PV system is influenced by the DC/DC converter, hitherto, no work has been done. In this paper, the configuration and mathematical models of PV system with and without DC/DC converter are studied deeply. Through comparing the difference of output parameters of two PV systems at the MPP, the bridge in connecting control signal and the PV panel parameters (V_m and I_m) is built to propose the new MPPT strategy, which is one of the main aims and innovations in this work.

In existing MPPT methods, there are some MPPT methods taking the changing weather conditions in account directly. A MPPT control method while searching for optimal parameters corresponding to weather conditions at that time has been proposed by Nobuyoshi Mutoh, etc. (Mutoh et al., 2006). A novel and fast MPPT method, through using parameter estimation to calculate the solar irradiance and temperature directly, has been proposed

Abbreviations: PV, photovoltaic; MPP, maximum power point; MPPT, maximum power point tracking; VWP, variable weather parameters; S, solar irradiance; T, PV panel temperature; R_L , load resistance or equivalent load resistance.

* Corresponding author at: School of Information Engineering, Hubei University for Nationalities, Enshi, China.

E-mail address: [xidur_surfer@163.com](mailto:xidu_surfer@163.com) (S. Li).

<http://dx.doi.org/10.1016/j.solener.2017.01.002>

0038-092X/© 2017 Elsevier Ltd. All rights reserved.

by Jen-Hao Teng, etc. (Teng et al., 2016). Meanwhile, in order to improve the MPPT speed as well as possible, some VWP methods have been proposed in Li (2015), Li et al. (2013, 2015). Their main advantages are the fast MPPT speed and strong adaptability for varying weather conditions and the key technique is to find out the relationship between control signal and VWP. In this paper, the VWP technique will be studied continuously and considered specially from the effect of the DC/DC converter on the MPP, which is also one of the main aims and innovations in this work.

There are also some MPPT methods using the PV panel parameters V_m and I_m . In paper (Pan et al., 1999), a linear current control is proposed on the basis of the linear relationship between I_m and the level of irradiance. In paper (Takashima et al., 2000), a feedback MPPT control method is proposed by computing from equations involving temperature and irradiance. However, these methods are used difficultly because of the variability and measurement of parameters V_m and I_m . In this paper, the direct relationship V_m or I_m and weather parameters (irradiance S and temperature T) is used successfully, which finds a direction to study new MPPT methods by using the PV panel parameters V_m and I_m .

When it comes to the MPPT control unit, the basic buck and boost DC/DC converters are usually used in most PV systems because of their simple structure and low cost (Li et al., 2015). Therefore, in this paper, PV system with boost DC/DC converter is selected to study new MPPT control strategy with VWP, and the conclusion on PV system with buck or buck/boost DC/DC converter can be analogy.

This paper is divided into the following sections: the configuration and mathematical models of PV system are studied, and the effect of the DC/DC converter on the MPP is analyzed in Section 2. The MPP difference between PV system with and without DC/DC converter is used to propose the new MPPT control strategy in Section 3. The implementation of proposed MPPT strategy is finished by finding out the relationship between MPP control signal and VWP in Section 4. The feasibility and availability of proposed MPPT strategy are verified, and the MPPT performance are analyzed and compared with P&O method and fuzzy method in Section 5. Some discussions are had in Section 6. Finally, some conclusions are drawn in Section 7.

2. Theoretical basis of proposed MPPT strategy

2.1. Configuration and mathematical models of PV system

The configuration of PV systems with DC/DC converter and without DC/DC converter can be shown in Figs. 1 and 2, respectively. Where V and I represent the output voltage and current of PV panel, respectively; V_o and I_o represent the output voltage and current of DC/DC converter, respectively; R_i represents the input resistance on the right of PV panel and R_L represent the load resistance or equivalent load resistance.

On the one hand, with respect to PV panel, its mathematical model in practical application can be simplified as Eq. (1) (Moura, 2009, Mutoh et al., 2006), and it has been used widely and is usually called as “Four-Parameter Model” whose basis is the one-diode model (Mutoh et al., 2006).

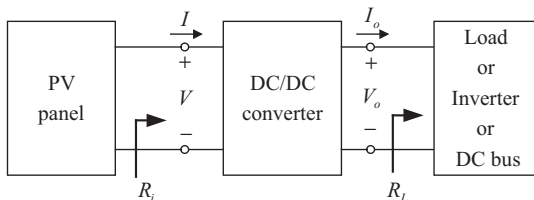


Fig. 1. Configuration of PV system with DC/DC converter.

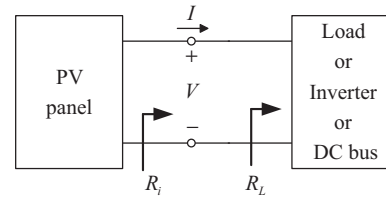


Fig. 2. Configuration of PV system without DC/DC converter.

$$I = I_{sc} \left[1 - C_1 \left(e^{\frac{V}{C_2 V_{oc}}} - 1 \right) \right] \quad (1)$$

where $C_1 = (1 - I_m/I_{sc}) \exp(-V_m/C_2 V_{oc})$; $C_2 = (V_m/V_{oc} - 1)/\ln(1 - I_m/I_{sc})$; I_{sc} , V_{oc} , I_m and V_m represent the short circuit current, the open circuit voltage, the MPP current and voltage at standard testing conditions (1000 W/m² and 25 °C), respectively. All data above are usually given by the PV array manufacturer.

On the other hand, according to Figs. 1 and 2, the input resistance R_i can be expressed as

$$R_i = \frac{V}{I} \quad (2)$$

In Fig. 1, the mathematical models of PV system can be described by the different equations corresponding to the different DC/DC converters. For example, according to paper (Enrique et al., 2007), R_i in Eq. (2) can be represented by Eqs. (3)–(5) when the DC/DC converters are the buck circuit, boost circuit and buck/boost circuit, respectively. Where D represents the duty cycle of PWM control signal of buck, boost or buck/boost DC/DC converter.

$$R_i = \frac{R_L}{D^2} \quad (3)$$

$$R_i = (1 - D)^2 R_L \quad (4)$$

$$R_i = \frac{(1 - D)^2}{D^2} R_L \quad (5)$$

Here, to make the theoretical analysis simple, PV system with boost DC/DC converter will be selected as the studied object. When the buck circuit or buck/boost circuit is selected as the DC/DC converter of PV system, the analogical conclusion can be drawn.

In Fig. 2, R_i in Eq. (2) can be represented by Eq. (6).

$$R_i = R_L \quad (6)$$

According to Eq. (4), it is known that R_i can be changed by the changing D or R_L , which is the MPPT principle of using boost DC/DC converter. Likewise, according to Eq. (6), R_i can also be changed by the changing R_L . However, in practical application, R_L need commonly keep constant, therefore, normally, PV system shown in Fig. 2 cannot operate at the MPP. In this paper, when the effect of the DC/DC converter to the MPP is analyzed, assume that the available R_L is selected to make PV system shown in Fig. 2 operating at the MPP, and that PV systems shown in Figs. 1 and 2 are all operating under the same irradiance and temperature conditions.

2.2. Analysis on the effect of the DC/DC converter to the MPP

In order to analyze the effect of the DC/DC converter to the MPP, firstly, the mathematical models of PV systems with and without DC/DC converter operating at the MPP should be studied, respectively.

On the one hand, when PV system shown in Fig. 1 with boost DC/DC converter is operating at the MPP, Fig. 1 can be replaced by Fig. 3. Where R_{iMPP} represents the input resistance at the MPP;

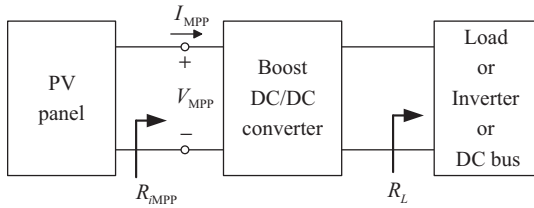


Fig. 3. Configuration of PV system with boost DC/DC converter operating at the MPP.

V_{MPP} and I_{MPP} represent the values of V and I corresponding to the MPP, respectively.

According to Fig. 3 and Eq. (2), Eq. (7) can be given.

$$R_{iMPP} = \frac{V_{MPP}}{I_{MPP}} \quad (7)$$

Meanwhile, according to Fig. 3, Eq. (4) can be represented by Eq. (8).

$$R_{iMPP} = (1 - D)^2 R_L \Big|_{MPP} = (1 - D_{max})^2 R_L \quad (8)$$

where D_{max} represents the duty cycle of PWM signal at the MPP for PV system with boost DC/DC converter. It is clear that Eqs. (7) and (8) are the mathematical models when PV system with boost DC/DC converter is operating at the MPP.

On the other hand, when PV system shown in Fig. 2 is just operating at the MPP, Fig. 2 can be replaced by Fig. 4. Where R_{im} represents the input resistance at the MPP now.

According to Fig. 4 and Eq. (2), Eq. (9) can be given.

$$R_{im} = \frac{V_m}{I_m} \quad (9)$$

It is clear that Eq. (9) is the mathematical model when PV system without DC/DC converter is just operating at the MPP.

Then, Fig. 5 can be given to show the MPP difference between PV system with and without DC/DC converter. Where the point A (V_{MPP} , I_{MPP}) represents the MPP of PV system with boost DC/DC converter; the point B (V_m , I_m) represents the MPP of PV system without DC/DC converter; l_1 and l_2 represent the characteristic lines of R_{iMPP} and R_{im} , respectively; α and β represent the input resistance angle corresponding to R_{iMPP} and R_{im} , respectively.

According to papers (Li et al., 2013 and Li et al., 2015), when PV system with DC/DC converter is operating at the MPP, Eq. (10) is just satisfied.

$$V_{MPP} = C \quad (10)$$

where C is a variable weather parameter whose value can be calculated by Eq. (11).

$$C = C_2 V_{oc} \left[\text{lambertw} \left(e \times \frac{1 + C_1}{C_1} \right) - 1 \right] \quad (11)$$

Because C is not equal to V_m at the MPP regardless of the topology of PV system with DC/DC converter, the points A and B do not coincide with each other, just as Fig. 5 has been showing. In fact, according to paper (Li, 2015), when the PV panel parameters I_{sc} ,

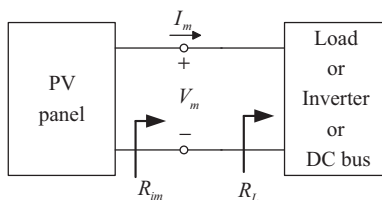


Fig. 4. Configuration of PV system without DC/DC converter operating at the MPP.

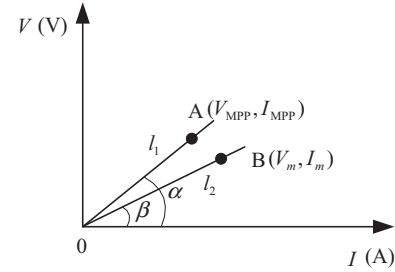


Fig. 5. MPP difference between PV system with and without DC/DC converter.

V_{oc} , I_m and V_m are selected as 9.19 A, 22 V, 8.58 A and 17.5 V at standard testing conditions, respectively, and the ideal DC/DC converter is used in simulation experiment, Eq. (12) is approximately satisfied.

$$V_{MPP} = V_m + 0.411 \quad (12)$$

Meanwhile, I_m and V_{MPP} are always greater than their corresponding I_{MPP} and V_m , respectively, under every given weather condition.

Finally, according to Fig. 5, Eqs. (13) and (14) can be given.

$$R_{iMPP} = \tan(\alpha) \quad (13)$$

$$R_{im} = \tan(\beta) \quad (14)$$

3. Proposition of proposed MPPT strategy

According to the analysis on the effect of the DC/DC converter to the MPP in Section 2.2, the MPP difference between PV system with and without DC/DC converter can be used to propose the new MPPT control strategy, which can be implemented by analyzing the MPPT control signal.

Firstly, assume that $R_{im} = R_{iMPP}$, according to Eqs. (8) and (9), Eq. (15) can be given

$$D_{max\ m} = 1 - \sqrt{\frac{V_m}{I_m R_L}} \quad (15)$$

where $D_{max\ m}$ represents the virtual duty cycle of PWM signal at the MPP if $R_{im} = R_{iMPP}$, and it can be regarded as the estimated value of D_{max} . The main aim using it is to find out the direct relationship between V_m , I_m and D_{max} .

Secondly, according to Fig. 5, the difference between R_{iMPP} and R_{im} can be defined as R_{iE} , and Eq. (16) can be given.

$$R_{iE} = R_{iMPP} - R_{im} = \tan(\alpha) - \tan(\beta) \quad (16)$$

Here, according to Eqs. (8), (9) and (16), Eq. (17) can be given

$$D_{max} = 1 - \sqrt{\frac{V_m + I_m R_{iE}}{I_m R_L}} \quad (17)$$

Thirdly, according to Eqs. (15) and (17), we assume that there is a relationship between $D_{max\ m}$ and D_{max} as shown in Eq. (18). Where $D_{max\ E}$ represents the error between $D_{max\ m}$ and D_{max} .

$$D_{max} = D_{max\ m} - D_{max\ E} \quad (18)$$

Eq. (18) can also be expressed as

$$D_{max\ E} = \frac{1}{\sqrt{R_L}} \left(\sqrt{\frac{V_m + I_m R_{iE}}{I_m}} - \sqrt{\frac{V_m}{I_m}} \right) \quad (19)$$

It can be clearly seen from Eq. (18) that the real-time control signal D_{max} can be given by the acquisition of $D_{max\ m}$ and $D_{max\ E}$, which is the principle of proposed MPPT strategy.

Finally, in order to propose the MPPT control strategy, Eq. (15) can be expressed as a function of R_L , S and T , and shown in Eq. (20).

$$D_{\max m} = f(S, T, R_L) \quad (20)$$

Meanwhile, Eq. (19) can also be expressed as a function of R_L , S and T , and shown in Eq. (21).

$$D_{\max E} = g(S, T, R_L) \quad (21)$$

According to Eqs. (18), (20) and (21), Eq. (22) can be given

$$D_{\max} = f(S, T, R_L) - g(S, T, R_L) \quad (22)$$

On the basis of Eq. (22), a new MPPT control strategy can be proposed and described as follows: PV system can operate around the MPP by controlling the duty cycle of DC/DC converter to equal to D_{\max} calculated by Eq. (22) after the parameters R_L , S and T have been measured.

4. Implementation of proposed MPPT strategy

On the one hand, to find out the relationship between $D_{\max m}$ and R_L , S , T , according to Eq. (15), the acquisition of parameters V_m and I_m are playing a key role. According to paper (Li, 2015), When the PV panel parameters I_{sc} , V_{oc} , I_m and V_m are selected as 9.19 A, 22 V, 8.58 A and 17.5 V, respectively, the mathematical relationship between V_m and S , T , can be expressed by Eq. (23).

$$\begin{aligned} V_m &= V_m(S, T) \\ &= 4.4 \times 10^{-6} \times (S - 638.25)^2 + 16.918 + 0.0504 \times (25 - T) \end{aligned} \quad (23)$$

Meanwhile, the mathematical relationship between I_m and S , T , can be expressed by Eq. (24).

$$\begin{aligned} I_m &= I_m(S, T) \\ &= 8.58 \times 10^{-3} \times S + (T - 25) \times 2.145 \times 10^{-5} \times S \end{aligned} \quad (24)$$

On the other hand, to find out the relationship between $D_{\max E}$ and R_L , S , T , Eq. (19) can be firstly replaced by Eq. (25).

$$M = D_{\max E} \times \sqrt{R_L} = \sqrt{\frac{V_m + I_m R_L}{I_m}} - \sqrt{\frac{V_m}{I_m}} \quad (25)$$

Then some simulation experiments are conducted by MATLAB software to find out the relationship between M and S , T , and experiment results can be shown in Fig. 6. Where Fig. 6 show the $M - S$ curves of PV system under various temperature conditions.

According to Fig. 6, the approximation function fitting $M - S$ curves can be given in Eq. (26) when T keeps varying.

$$\begin{aligned} M &= M(S, T) \\ &= -3.0825 \times 10^{-11} S^3 + 1.4033 \times 10^{-7} S^2 - 1.9627 \\ &\quad \times 10^{-4} S + 0.11683 + 2 \times 10^{-7} \times (25 - T)(S - 750) \end{aligned} \quad (26)$$

After these relationships shown in Eqs. (23), (24) and (26) have been found out, Eq. (22) can be epitomized as Eq. (27).

$$D_{\max} = 1 - \sqrt{\frac{V_m(S, T)}{I_m(S, T) \times R_L}} - \frac{M(S, T)}{\sqrt{R_L}} \quad (27)$$

It is clear that the relationship shown in Eq. (27) can ensure the control signal D_{\max} calculated out successfully after the parameters R_L , S and T have been measured, which plays the key role in the implementation of proposed MPPT control strategy.

Meanwhile, according to the above description of proposed MPPT control strategy and Eq. (27), to ensure PV system operating at MPP, the real-time value of duty cycle D_{\max} should be calculated out by MPPT controller. Meanwhile, Eq. (27) also shows that the

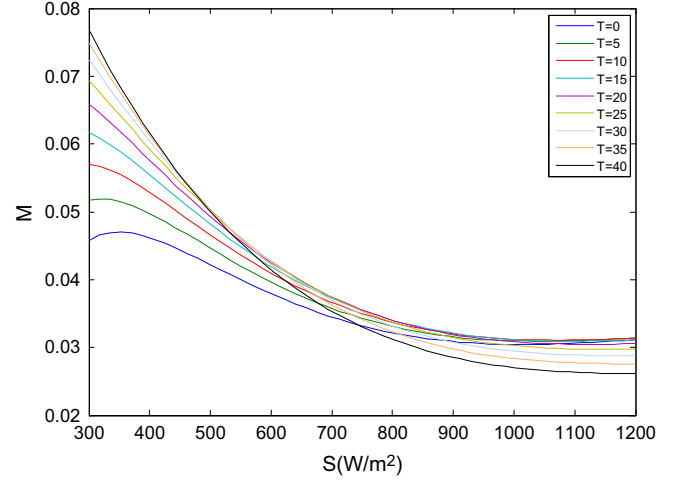


Fig. 6. $M - S$ curves under various T conditions.

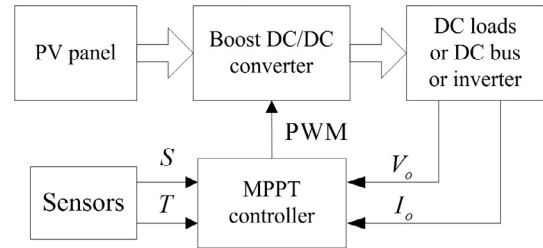


Fig. 7. Structure of PV system controlled by proposed MPPT strategy.

calculation of D_{\max} needs to take sample not only S and T but also V_o and I_o . Therefore, the structure of PV system to implement this proposed MPPT strategy can be designed and shown in Fig. 7.

5. Simulation experiments and results analysis

When the proposed MPPT control strategy is used, in order to verify its feasibility and availability, and test the MPPT performance of PV system, many simulation experiments whose circuit structure is shown in Fig. 7 are conducted by MATLAB. Where PV panel model whose parameters are the same as Section 2.2 is built by Simulink according to Eq. (1); For boost DC/DC converter, the inductance and capacitor whose values are 1.5mH and 2200uF, respectively, are all ideal components; IGBT with 1 m Ω internal resistance is chosen as the switch, and the internal resistance and forward voltage of the diode are 1 m Ω and 0.8 V, respectively; the frequency of PWM control signal is 20 kHz; the conventional P&O method whose tracking step size is 0.003 is selected as the compared object; assume a load resistance 20 Ω is connected with boost DC/DC converter in Fig. 7.

5.1. Feasibility and availability experiments of proposed MPPT strategy

5.1.1. Experiments under given arbitrary weather conditions

When it is comes the verification of the feasibility and availability of proposed MPPT control strategy, the experiment results are shown in Table 1 under various weather conditions. In Table 1, P_{\max} and D_{\max} represent the ideal values of output power and duty cycle corresponding to the MPP, respectively; P_{\max}^* and D_{\max}^* represent the experiment results of output power and duty cycle corresponding to the MPP, respectively, when the proposed MPPT strategy is used; $P_{\max\%}^*$ and $D_{\max\%}^*$ represent the experiment results

Table 1
Experimental results under various weather conditions.

(S, T)(W/m ² , °C)	D_{max}	D_{max}^*	$D_{max,k}^*$	P_{omax} (W)	P_{omax}^* (W)	$P_{omax,k}^*$ (W)
(300,0)	0.3654	0.3628	0.365	44.81	42.11	42.10
(300,10)	0.3812	0.3790	0.381	45.14	42.07	42.06
(300,20)	0.3971	0.3949	0.397	44.98	41.96	41.96
(500,0)	0.5136	0.5126	0.513	72.94	70.35	70.32
(500,10)	0.5265	0.5253	0.526	73.37	70.28	70.26
(500,20)	0.5393	0.5376	0.540	73.01	70.10	70.07
(800,10)	0.6253	0.6255	0.6255	116.64	114.54	114.50
(800,20)	0.6352	0.6353	0.636	116.30	114.26	114.20
(800,30)	0.6449	0.6450	0.645	116.84	113.82	113.74
(1000,20)	0.6685	0.6696	0.669	148.73	147.76	147.65
(1000,30)	0.6781	0.6783	0.678	149.93	147.19	147.05
(1000,40)	0.6862	0.6868	0.687	149.44	146.40	146.25
(1200,20)	0.6903	0.6911	0.690	188.94	186.42	186.20
(1200,30)	0.6993	0.6991	0.699	186.15	185.70	185.50
(1200,40)	0.7068	0.7070	0.708	186.11	184.70	184.45

of output power and duty cycle corresponding to the MPP, respectively, when the P&O method is used.

It can be seen from Table 1 that the errors between every D_{max}^* and its corresponding D_{max} are always less than 0.3%, and the errors between every D_{max}^* and its corresponding $D_{max,k}^*$ are always less than 0.3%, which means that the value of D_{max}^* is approximately equal to its corresponding D_{max} or $D_{max,k}^*$ under a certain weather condition. Meanwhile, It can be also seen from Table 1 that, under a given weather condition, P_{omax}^* is approximately equal to its corresponding P_{omax} and the errors between them are always less than 0.3 W, and that there is a small difference between P_{omax} and P_{omax}^* or $P_{omax,k}^*$ because of the nonideal boost DC/DC converter and measurement error. Although this difference is existing, according to these experiment results, a conclusion can be still drawn that the proposed MPPT method is feasible and available in controlling successfully PV system to operate around the MPP.

Moreover, in Table 1, the results of $D_{max,k}^*$ and $P_{omax,k}^*$ are all the average values because of the output oscillation of P&O method. Meanwhile, because the MPPT accuracy is influenced by the tracking step size 0.003 of P&O method, $P_{omax,k}^*$ is usually smaller than its corresponding P_{omax}^* under every weather condition.

5.1.2. Experiments for testing the errors between D_{max}^* and D_{max}

In Section 5.1.1, the feasibility and availability of proposed MPPT control strategy have been directly verified under given arbitrary weather conditions. Here, some experiments will be conducted to verifies indirectly its feasibility and availability by testing the error between D_{max}^* and D_{max} , and the experiment results are shown in Figs. 8–10. Meanwhile, to make the shown experiment results clearer, the parameter $D_{mE}\%$, which can be called as the error percentage between D_{max}^* and D_{max} , is defined

$$D_{mE}\% = \frac{D_{max}^* - D_{max}}{D_{max}} \times 100\%. \tag{28}$$

Figs. 8, 9 and 10 show the $D_{mE}\% - S$, $D_{mE}\% - T$ and $D_{mE}\% - R_L$ curves under 25 °C and 20 Ω, 1000 W/m² and 20 Ω, and 1000 W/m² and 25 °C conditions, respectively.

It can be clearly seen from Fig. 8 that the error percentage $D_{mE}\%$ is always less than 0.055% under 25 °C, 20 Ω and various S conditions. Meanwhile, Fig. 9 shows that the error percentage $D_{mE}\%$ is always less than 0.03% under 1000 W/m², 20 Ω and various T conditions. Finally, Fig. 10 shows that the error percentage $D_{mE}\%$ is always less than 0.015% under 1000 W/m², 25 °C and various R_L conditions. According to these results, it is clear that the calculated values D_{max}^* by MPPT controller using the proposed MPPT strategy are always approximately equal to their corresponding ideal values

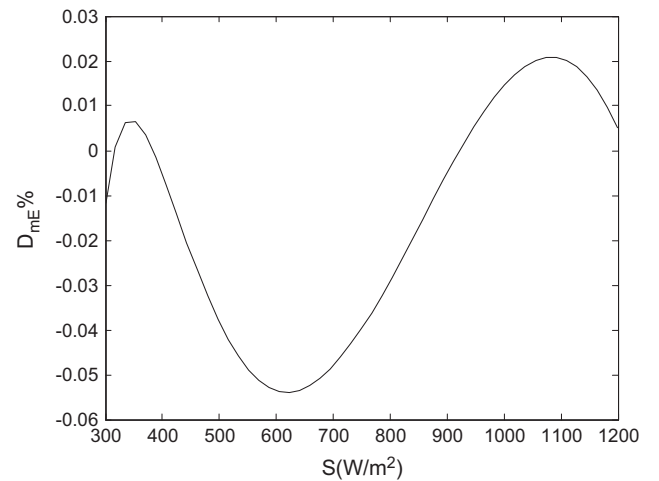


Fig. 8. $D_{mE}\% - S$ curves under 25 °C and 20 Ω conditions.

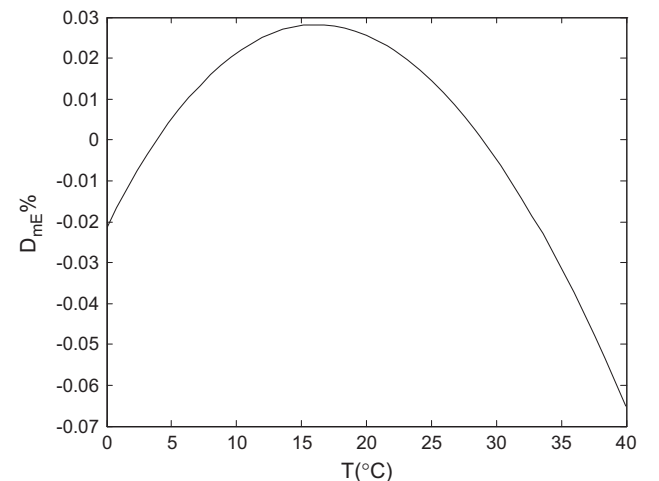


Fig. 9. $D_{mE}\% - T$ curves under 1000 W/m² and 20 Ω conditions.

D_{max} regardless of various S, T and R_L , which means that PV system can always operate around the MPP.

According to these experiment results and analysis in this Section, a conclusion can be drawn that the proposed MPPT control strategy is feasible and available in controlling successfully PV system to operate around the MPP.

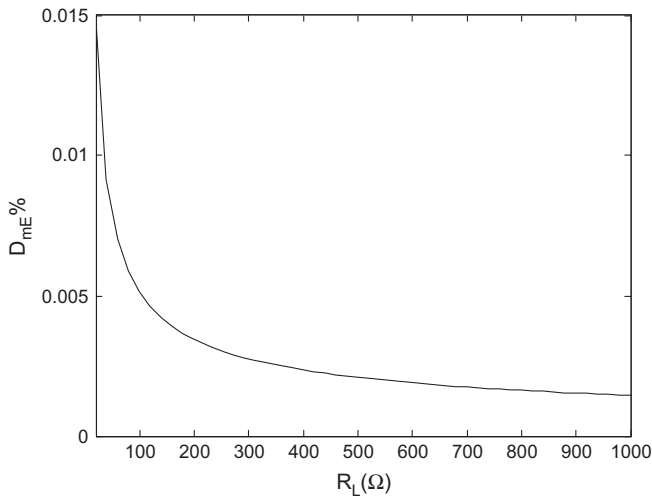


Fig. 10. $D_{mE}\%$ – R_L curves under 1000 W/m^2 and $25 \text{ }^\circ\text{C}$ conditions.

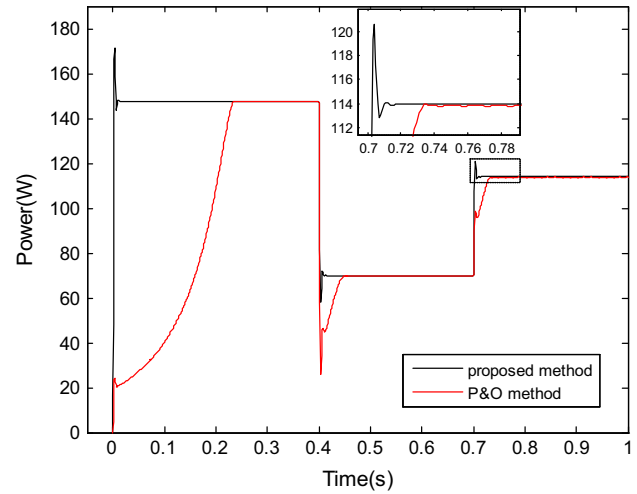


Fig. 11. Compared power curves under ① conditions.

5.2. Analysis of MPPT performance

To analyze the MPPT performance of proposed MPPT control strategy, some experiments are also conducted by MATLAB. In these experiments, PV system is assumed to operate under ① invariable T and variable S , ② invariable S and variable T , and ③ variable S and T conditions, respectively. Here, to make a MPPT performance comparison between proposed MPPT strategy and conventional P&O method, their output power curves or duty cycle curves are shown together in all following figures. Meanwhile, in these experiment results, t_s^* and t_{sk}^* represent the settling times corresponding to the proposed strategy and P&O method, respectively; P_{omax}^* and P_{omaxk}^* represent the output powers corresponding to the proposed strategy and P&O method, respectively; D_{max}^* and D_{maxk}^* represent the duty cycles corresponding to the proposed strategy and P&O method, respectively.

5.2.1. Experiments under invariable T and variable S conditions

When S is varying and T keeps at $25 \text{ }^\circ\text{C}$, an experiment is done and the experiment results are shown in Figs. 11 and 12. In this experiment, the changing values of S and their corresponding ranges of time are shown in Table 2 and the experiment results corresponding to Figs. 11 and 12 are shown in Table 3. Meanwhile, to compare and analyze the experiment results easily, the key ideal values (D_{max} and P_{omax}) corresponding to every weather condition are also shown in Table 2 and the experiment results for P&O method are also shown in Figs. 11 and 12.

Compare the data in Table 2 with Table 3, it is clearly known that PV system can always operate around MPP when the proposed MPPT strategy or P&O method is used under $T = 25 \text{ }^\circ\text{C}$ and variable S conditions. Meanwhile, Combine Fig. 11 with Table 3, we know that the settling times of proposed MPPT strategy are far less than those of P&O method in every time interval. That is to say, the rapidity of proposed MPPT strategy is far better than that of P&O method under $T = 25 \text{ }^\circ\text{C}$ and variable S conditions. It is obvious that this conclusion can also be drawn by combining Fig. 12 with Table 3. Lastly, Fig. 11 and Fig. 12 also show that the proposed MPPT control strategy makes the output power and duty cycle stabilize at the MPP while the P&O method makes them oscillating around the MPP under $T = 25 \text{ }^\circ\text{C}$ and variable S conditions.

According to the above-mentioned experiment results and corresponding analysis, a conclusion can be drawn that, under invariable T and variable S conditions, PV system using proposed MPPT control strategy can always operate around MPP and has better

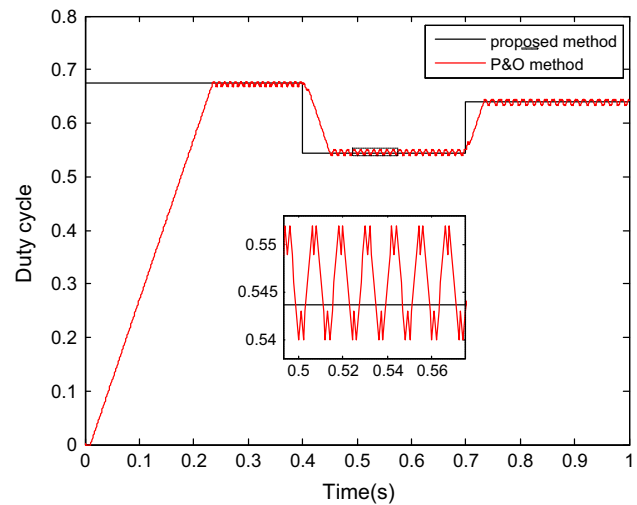


Fig. 12. Compared duty cycle curves under ① conditions.

Table 2
Values of experimental parameters under $T = 25 \text{ }^\circ\text{C}$ condition.

Weather conditions and key ideal values	Range of time (s)		
	From 0 to 0.4	From 0.4 to 0.7	From 0.7 to 1
$S \text{ (W/m}^2\text{)}$	1000	500	800
D_{max}	0.6733	0.5452	0.6403
$P_{omax} \text{ (W)}$	149.54	72.56	116.74

Table 3
Experimental results corresponding to Figs. 11 and 12.

Experiment results	Range of time (s)		
	From 0 to 0.4	From 0.4 to 0.7	From 0.7 to 1
$P_{omax}^* \text{ (W)}$	147.51	69.98	113.91
$P_{omaxk}^* \text{ (W)}$	147.42	69.95	113.80
$t_s^* \text{ (ms)}$	20	21	18
$t_{sk}^* \text{ (ms)}$	236	52	35
D_{max}^*	0.6740	0.5437	0.6400
D_{maxk}^*	0.6735	0.546	0.639

MPPT transient-state and steady-state performance than conventional P&O method.

5.2.2. Experiments under invariable S and variable T conditions

When T is varying and S keeps at 1000 W/m^2 , an experiment is also done and the experiment results are shown in Figs. 13 and 14. In this experiment, the changing values of T and their corresponding ranges of time are shown in Table 4. Meanwhile, to compare and analyze the experiment results easily, the key ideal values (D_{\max} and P_{omax}) corresponding to every weather condition are also shown in Table 4 and the experiment results for P&O method are also shown in Figs. 13 and 14.

Compare the data in Table 4 with Table 5, it is clearly known that PV system can always operate around MPP when the proposed MPPT strategy or P&O method is used under $S = 1000 \text{ W/m}^2$ and variable T conditions. Meanwhile, Combine Fig. 13 with Table 5, we know that the settling times of proposed MPPT strategy are far less than those of P&O method in every time interval. That is to say, the rapidity of proposed MPPT strategy is far better than that of P&O method under $S = 1000 \text{ W/m}^2$ and variable T conditions. It is obvious that this conclusion can also be drawn by combining Fig. 14 with Table 5. Lastly, Fig. 13 and Fig. 14 also show that the proposed MPPT control strategy makes the output power and duty cycle stabilize at the MPP while the P&O method makes them oscillating around the MPP under $S = 1000 \text{ W/m}^2$ and variable T conditions.

According to the above-mentioned experiment results and corresponding analysis, a conclusion can be drawn that, under invariable S and variable T conditions, PV system using proposed MPPT control strategy can always operate around MPP and has better MPPT transient-state and steady-state performance than conventional P&O method.

5.2.3. Experiments under variable S and T conditions

When both T and S are varying, an experiment is also done and the experiment results are shown in Figs. 15 and 16. In this experiment, the changing values of T and S are shown in Table 6. Meanwhile, to compare and analyze the experiment results easily, the key ideal values (D_{\max} and P_{omax}) corresponding to every weather condition are also shown in Table 6 and the experiment results for P&O method are also shown in Figs. 15 and 16.

Compare the data in Table 6 with Table 7, it is clearly known that PV system can always operate around MPP when the proposed MPPT strategy or P&O method is used under variable S and T con-

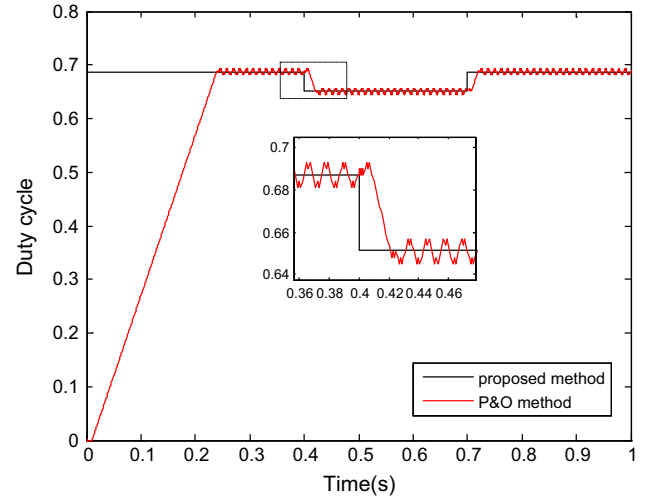


Fig. 14. Compared duty cycle curves under ② conditions.

Table 4

Values of experimental parameters under $S = 1000 \text{ W/m}^2$ condition.

Weather conditions and key ideal values	Range of time (s)		
	From 0 to 0.4	From 0.4 to 0.7	From 0.7 to 1
T ($^{\circ}\text{C}$)	40	0	40
D_{\max}	0.6862	0.6503	0.6862
P_{omax} (W)	149.44	151.31	149.44

Table 5

Experimental results corresponding to Figs. 13 and 14.

Experiment results	Range of time (s)		
	From 0 to 0.4	From 0.4 to 0.7	From 0.7 to 1
P_{omax}^+ (W)	146.40	148.26	146.40
P_{omax}^* (W)	146.25	148.15	146.25
t_s^+ (ms)	19	10	14
t_{sk}^+ (ms)	240	22	20
D_{max}^*	0.6868	0.6516	0.6868
D_{max}^*	0.687	0.651	0.687

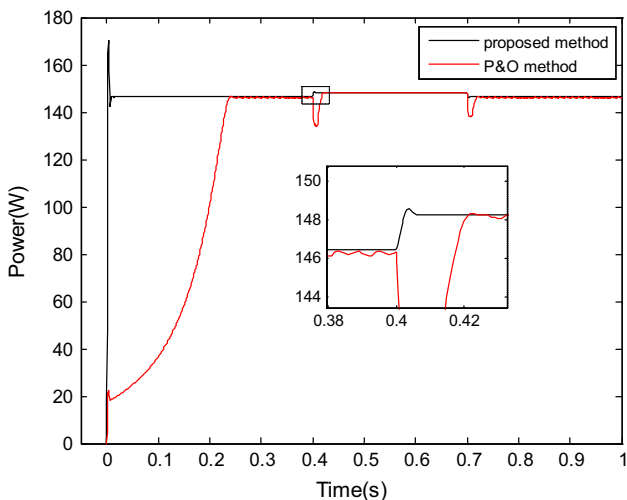


Fig. 13. Compared power curves under ② conditions.

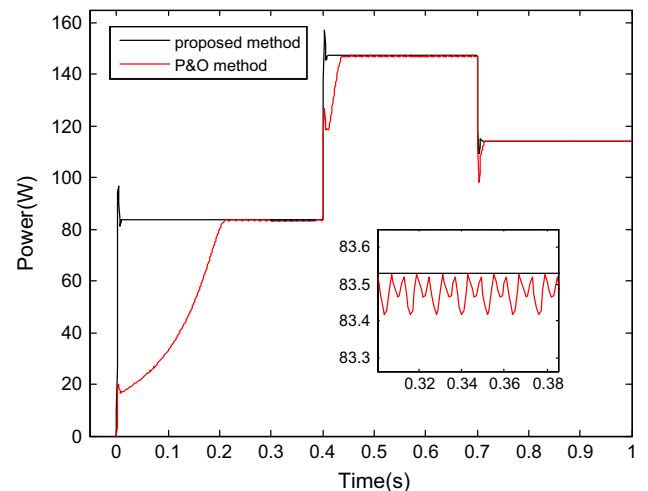


Fig. 15. Compared power curves under ③ conditions.

ditions. Meanwhile, Combine Fig. 15 with Table 7, we know that the settling times of proposed MPPT strategy are less than those of P&O method in every time interval. That is to say, the rapidity of proposed MPPT strategy is better than that of P&O method under variable S and T conditions. It is obvious that this conclusion can also be drawn by combining Fig. 16 with Table 7. Lastly, Fig. 15 and Fig. 16 also show that the proposed MPPT control strategy makes the output power and duty cycle stabilize at the MPP while the P&O method makes them oscillating around the MPP under variable S and T conditions.

According to the above-mentioned experiment results and corresponding analysis, a conclusion can be drawn that, under variable S and T conditions, PV system using proposed MPPT control strategy can always operate around MPP and has better MPPT transient-state and steady-state performance than conventional P&O method.

In sum, according to all experiment results and corresponding analysis in Sections 5.2.1, 5.2.2 and 5.2.3, the conclusion can be drawn that, under various weather conditions, PV system can be controlled to operate around its MPP by using proposed MPPT control strategy and the MPPT performance are better than P&O method.

5.3. Comparison with other MPPT methods

To make a comparison between proposed MPPT strategy and other MPPT methods, an experiment is done by MATLAB under fast changing weather conditions. Here, the fuzzy method in paper (Bouchafaa et al., 2011) and conventional P&O method are selected as the compared objects in this experiment, and the tracking step size of P&O method is selected as 0.003. Meanwhile, assume that the solar irradiance changes according to Fig. 17 when the temperature and load resistance keep at 25 °C and 200 Ω, respectively. Finally, the experiment result is shown in Fig. 18. Moreover, to judge whether PV system is operating at the MPP, the ideal MPP values with varying irradiance (represented by ideal MPP) are also shown in Fig. 18.

It can be clearly seen from Fig. 18 that, firstly, all three MPPT methods can track the MPP successfully while there is a MPPT failure of P&O method within 0.2 s because of its slow tracking speed. Secondly, the settling time of proposed strategy is always better than fuzzy method and P&O method. Thirdly, the output power of proposed strategy can be stabilized at the MPP while there is some oscillation around the MPP for P&O method or fuzzy method.

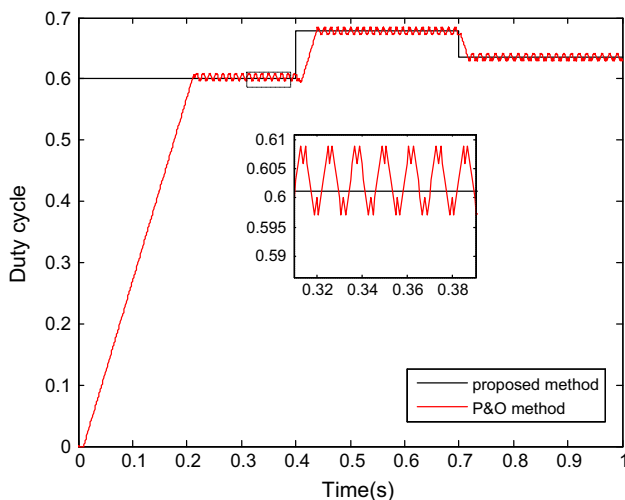


Fig. 16. Compared duty cycle curves under © conditions.

Table 6
Values of experimental parameters under variable S and T conditions.

Weather conditions and key ideal values	Range of time (s)		
	From 0 to 0.4	From 0.4 to 0.7	From 0.7 to 1
S (W/m ²)	600	1000	800
T (°C)	40	30	20
D_{max}	0.6024	0.6781	0.6352
P_{omax} (W)	86.36	149.93	116.30

Table 7
Experimental results corresponding to Figs. 15 and 16.

Experiment results	Range of time (s)		
	From 0 to 0.4	From 0.4 to 0.7	From 0.7 to 1
P_{omax}^* (W)	83.53	147.19	114.11
P_{omaxk}^* (W)	83.48	147.05	114.02
t_s^* (ms)	20	17	17
t_{sk}^* (ms)	212	40	20
D_{max}^*	0.6012	0.6783	0.6349
D_{maxk}^*	0.603	0.678	0.636

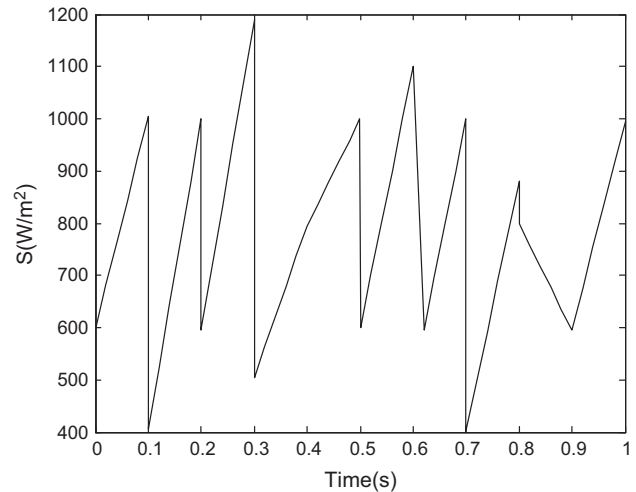


Fig. 17. Changing curve of S in the simulation experiment.

In sum, a conclusion can be drawn by this simulation experiment that the proposed control strategy has better MPPT performance than other two methods under fast changing weather conditions. That is to say, PV system using the proposed control strategy has the better adaptability to fast changing weather conditions.

6. Discussions

Firstly, there may be some errors in using curve-fitting technique to find out the relationship between V_m (I_m or M) and S , T . However, there is a small influence on MPPT performance according to experiment results in Section 5. If we must decrease these errors, some ways can be used as follows. On the one hand, the curve-fitting technique should focus on the main working area (irradiance range or temperature range) of PV system to ensure the accuracy. On the other hand, a correction term can be used to rectify these curve-fitting errors.

Secondly, the accuracy, rapidity and stability of P&O method or fuzzy method are usually influenced by its MPPT step size. The bigger its step size is, the better its MPPT rapidity is while the poorer

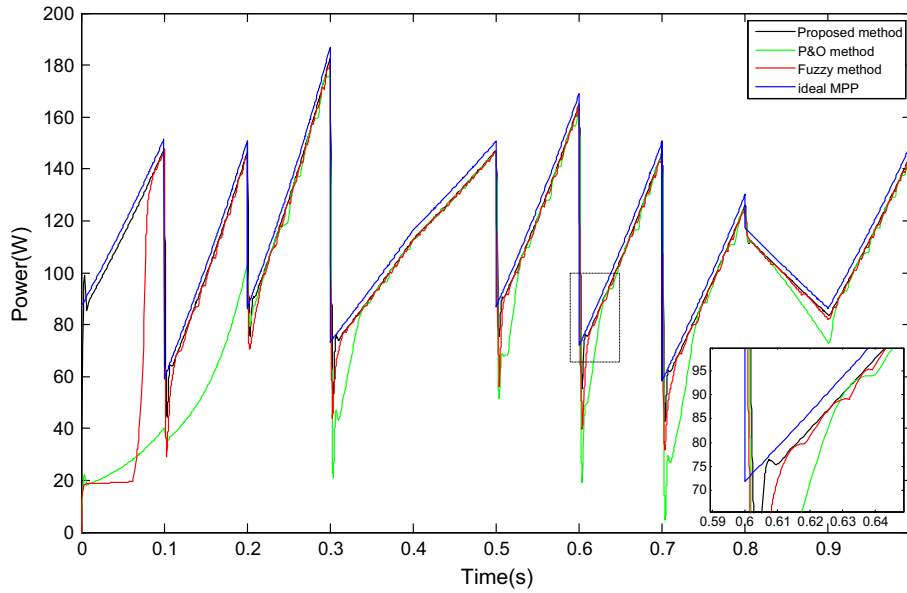


Fig. 18. Compared output power curves by using three MPPT methods.

Table 8
Experimental results with measurement error.

(S, T) (W/m ² , °C)	(300,10)	(500,15)	(500,20)	(800,10)	(800,20)	(1000,20)	(1000,30)
P_{omax}^{T+} (W)	42.05	70.17	70.06	114.50	114.19	147.67	147.05
P_{omax}^{T-} (W)	42.08	70.24	70.15	114.58	114.33	147.85	147.32
P_{omax}^{S+} (W)	42.78	70.91	70.81	115.33	115.05	148.66	148.09
P_{omax}^{S-} (W)	41.35	69.50	69.40	113.75	113.48	146.87	146.30
$P_{\text{omax}}^{S+5\%}$ (W)	44.20	73.74	73.63	120.91	120.62	156.89	156.28
$P_{\text{omax}}^{S-5\%}$ (W)	39.92	66.68	66.59	108.31	108.05	138.96	138.42
P_{omax}^* (W)	42.07	70.20	70.10	114.54	114.26	147.76	147.19
P_{omax} (W)	45.14	73.28	73.01	116.64	116.30	148.73	149.93

its MPPT accuracy is and the bigger the output power oscillation around the MPP is. In this paper, the rapidity and accuracy are all considered comprehensively, so the P&O method with step size 0.003 has been selected as compared object in all experiments. Meanwhile, it can be seen from Fig. 18 that the fuzzy method has better MPPT performance than P&O method because of its variable step size.

Thirdly, Eqs. (23), (24) and (26) have been determined by simulation experiments for PV system with boost DC/DC converter when the PV panel parameters I_{sc} , V_{oc} , I_m and V_m are selected as 9.19 A, 22 V, 8.58 A and 17.5 V, respectively. In practical application, on the one hand, when the four panel parameters are different from these values, we can find out easily the corresponding equations to match different PV panel parameters by some simulation experiments, and build a list for user. On the other hand, for PV system with buck or buck/boost DC/DC converter, to make the proposed MPPT strategy available, Eqs. (25)–(27) must be all replaced. For example, for PV system with buck DC/DC converter, Eqs. (25)–(27) must be replaced by Eqs. (29)–(31), respectively.

$$M = \frac{D_{\text{max}} E}{\sqrt{R_L}} = \sqrt{\frac{I_m}{V_m}} - \sqrt{\frac{I_m}{V_m + I_m R_{IE}}} \quad (29)$$

$$M = M(S, T) = 2.1199 \times 10^{-11} S^3 - 4.8147 \times 10^{-8} S^2 + 4.09 \times 10^{-5} S + 8.76 \times 10^{-5} + 1.2 \times 10^{-4} \times (T - 15) \quad (30)$$

$$D_{\text{max}} = \sqrt{\frac{I_m(S, T) \times R_L}{V_m(S, T)}} - \sqrt{R_L} \times M(S, T) \quad (31)$$

Finally, in order to conduct the sensitivity analysis of the utilized parameters, including solar irradiance (S) and cell temperature (T), some simulation experiments are done and experiment results are shown in Table 8. Where P_{omax}^{T+} and P_{omax}^{T-} represent the output power values of using the proposed MPPT strategy when the measured data of T have the error of +2°C and -2°C, respectively. P_{omax}^{S+} and P_{omax}^{S-} represent the output power values of using the proposed MPPT strategy when the measured data of S have the error of +5W/m² and -5W/m², respectively. $P_{\text{omax}}^{S+5\%}$ and $P_{\text{omax}}^{S-5\%}$ represent the output power values of using the proposed MPPT strategy when the measured data of S have the error of +5% and -5%, respectively. P_{omax} represents the ideal output power without measurement error and P_{omax}^* represents the output power of using the proposed MPPT strategy without measurement error.

It can be seen from Table 8 that the errors between P_{omax}^{T+} or P_{omax}^{T-} and P_{omax}^* are always less than 0.15 W, which means that the output power of PV system is almost unaffected by the small measurement error of T. Meanwhile, it can be also seen from Table 8 that the errors between P_{omax}^{S+} or P_{omax}^{S-} and P_{omax}^* are always less than 0.9 W, which also means that the output power of PV system is almost unaffected by the small measurement error of S. In addition, it can be also seen from Table 8 that the errors between $P_{\text{omax}}^{S+5\%}$ or $P_{\text{omax}}^{S-5\%}$ and P_{omax}^* are always less than 10 W (or 6.2%), which

means that some effect on the output power of PV system is had by the irradiance measurement error of 5%.

7. Conclusions

In this paper, through analyzing the effect of the DC/DC converter to the MPP of PV system, a MPPT control strategy with VWP, which has the ability to track the MPP more rapidly, has been proposed. In this study, the key work is to find out the way for acquiring the control signal at the MPP through analyzing deeply the difference between PV system with and without DC/DC converter. Meanwhile, the acquisition of mathematical relationship between control signal and VWP is also playing a key role to implement this proposed MPPT strategy. Finally, by simulation experiments, the feasibility and availability of this proposed control strategy have been verified, and the MPPT performance of this proposed control strategy has been analyzed under different weather conditions and has been compared with fuzzy method and P&O method under fast varying irradiance conditions.

Acknowledgements

This work was supported by guidance project of Hubei Provincial Department of Education (No. B2016494), National Natural Science Foundation of China (No. 61463014) and scientific research project of Science and Technology College of Hubei University for Nationalities (No. KJB201601).

References

- Ahmed, Jubaer, Salam, Zainal, 2015. An improved perturb and observe maximum power point tracking algorithm for higher efficiency. *Appl. Energy* 150, 97–108.
- Bouchafaa, F., Hamzaoui, I., Hadjammam, A., 2011. Fuzzy logic control for the tracking of maximum power point of a PV system. *Energy Procedia* 6, 633–642.
- Deshkar, Shubhankar Niranjana, Dhale, Sumedh Bhaskar, Mukherjee, Jishnu Shekar, et al., 2015. Solar PV array reconfiguration under partial shading conditions for maximum power extraction using genetic algorithm. *Renew. Sustain. Energy Rev.* 43, 102–110.
- Elgendy, Mohammed A., Zahawi, Bashar, Atkinson, David J., 2013. Assessment of the incremental conductance maximum power point tracking algorithm. *IEEE Trans. Sustain. Energy* 4 (1), 108–117.
- Enrique, J.M., Durán, E., Sidrach-de-Cardona, M., Andújar, J.M., 2007. Theoretical assessment of the maximum power point tracking efficiency of photovoltaic facilities with different converter topologies. *Sol. Energy* 81, 31–38.
- Guenounou, Ouahib, Dahhou, Boutaib, Chabour, Ferhat, 2014. Adaptive fuzzy controller based MPPT for photovoltaic systems. *Energy Convers. Manage.* 78, 843–850.
- Hong, Chih-Ming, Chen, Chiung-Hsing, 2014. Intelligent control of a grid-connected wind-photovoltaic hybrid power systems. *Electr. Power Energy Syst.* 55, 554–561.
- Ishaque, Kashif, Salam, Zainal, Lauss, George, 2014. The performance of perturb and observe and incremental conductance maximum power point tracking method under dynamic weather conditions. *Appl. Energy* 119, 228–236.
- Jiang, Joe-Air, Su, Yu-Li, Shieh, Jyh-Cherng, et al., 2014. On application of a new hybrid maximum power point tracking based photovoltaic system to the closed plant factory. *Appl. Energy* 124, 309–324.
- Li, Shaowu, 2015. A maximum power point tracking method with variable weather parameters based on input resistance for photovoltaic system. *Energy Convers. Manage.* 106, 290–299.
- Li, Shaowu, Gao, Xianwen, Wang, Lina, Liu, Sanjun, 2013. A novel maximum power point tracking control method with variable weather parameters for photovoltaic systems. *Sol. Energy* 97, 529–536.
- Li, Shaowu, Attou, Amine, Yang, Yongchao, Geng, Dongshan, 2015. A maximum power point tracking control strategy with variable weather parameters for photovoltaic systems with DC bus. *Renew. Energy* 74, 478–488.
- Liu, Yali, Li, Ming, Ji, Xu, et al., 2014. A comparative study of the maximum power point tracking methods for PV systems. *Energy Convers. Manage.* 85, 809–816.
- Mellit, Adel, Kalogirou, Soteris A., 2014. MPPT-based artificial intelligence techniques for photovoltaic systems and its implementation into field programmable gate array chips: review of current status and future perspectives. *Energy* 70, 1–21.
- Mohanty, Parimita, Bhuvaneshwari, G., Balasubramanian, R., Dhaliwal, Navdeep Kaur, 2014. MATLAB based modeling to study the performance of different MPPT techniques used for solar PV system under various operating conditions. *Renew. Sustain. Energy Rev.* 38, 581–593.
- Moura, Scott., 2009. A switched extremum seeking approach to maximum power point tracking in photovoltaic systems. *Grid Integr. Altern. Energy Sour.*, 1–17.
- Mutoh, Nobuyoshi, Ohno, Masahiro, Inoue, Takayoshi, 2006. A method for MPPT control while searching for parameters corresponding to weather conditions for PV generation systems. *IEEE Trans. Industr. Electron.* 53 (4), 1055–1065.
- Mutoh, Nobuyoshi, Ohno, Masahiro, Inoue, Takayoshi, 2006. A method for MPPT control while searching for parameters corresponding to weather conditions for PV generation systems. *IEEE Trans. Ind. Electron.* 53 (4), 1055–1065.
- Pan, Ching-Tsai, Chen, Jeng-Yue, Chu, Chin-Peng, Huang, Yi-Shuo, 1999. A fast maximum power point tracker for photovoltaic power systems. In: *Proc. 25th Annu. Conf. IEEE Ind. Electron. Soc.*, pp. 390–393.
- Salam, Zainal, Ahmed, Jubaer, Merugu, Benny S., 2013. The application of soft computing methods for MPPT of PV system: a technological and status review. *Appl. Energy* 107, 135–148.
- Shaiek, Yousra, Smida, Mouna Ben, Sakly, Anis, Mimouni, Mohamed Faouzi, 2013. Comparison between conventional methods and GA approach for maximum power point tracking of shaded solar PV generators. *Sol. Energy* 90, 107–122.
- Sivakumar, P., Kader, Abdullah Abdul, Kaliavaradhan, Yogeshraj, Arutchelvi, M., 2015. Analysis and enhancement of efficiency with incremental conductance MPPT technique under non-linear loading conditions. *Renew. Energy* 81, 543–550.
- Takashima, T., Tanaka, T., Amano, M., Ando, Y., 2000. Maximum output control of photovoltaic (PV) array. In: *Proc. 35th Intersociety Energy Convers. Eng. Conf. Exhib.*, pp. 380–383.
- Teng, Jen-Hao, Huang, Wei-Hao, Hsu, Tao-An, Wang, Chih-Yen, 2016. Novel and fast maximum power point tracking for photovoltaic generation. *IEEE Trans. Industr. Electron.* 63 (8), 4955–4966.
- Tsang, K.M., Chan, W.L., 2013. Model based rapid maximum power point tracking for photovoltaic systems. *Energy Convers. Manage.* 70, 83–89.
- Zhang, Fan, Maddy, Jon, Premier, Giuliano, Guwy, Alan, 2015. Novel current sensing photovoltaic maximum power point tracking based on sliding mode control strategy. *Sol. Energy* 118, 80–86.